JOURNAL OF Materials CHEMISTRY

2-Mercaptobenzothiazole protected Au and Ag clusters

N. Sandhyarani and T. Pradeep*

Department of Chemistry and Regional Sophisticated Instrumentation Centre, Indian Institute of Technology, Madras 600 036, India. E-mail: pradeep@acer.iitm.ernet.in

Received 16th November 1999, Accepted 12th January 2000
Published on the Web 22nd February 2000

Nanometer sized gold and silver clusters protected with 2-mercaptobenzothiazole monolayers have been prepared and characterized by various spectroscopic methods. Optical absorption spectra show features assigned to charge-transfer excitation between the monolayer and the cluster, in addition to a red shifting and reduction of plasmon absorption. The monolayers on clusters are compared with the corresponding 2D-monolayers investigated previously. The dominant adsorbate geometries on these clusters are different. Whereas the temperature dependent dynamics are minimal for 2D-SAMs, they are significant for monolayers on 3D surfaces, which is attributed to the decreased packing density on the cluster surfaces. The thermal stability of these monolayers is high and comparable to that of alkanethiolate monolayers. The monolayers undergo irreversible structural changes upon heating, which have been studied by differential scanning calorimetry and IR spectroscopy.

Introduction

The synthesis, characterization and properties of self-organized structures of nanomaterials have become an active area of research in the last few years. Their unique physical and chemical properties give rise to a variety of applications such as sensors, catalysts, nanoelectronic devices and more.[1] Recently it was reported that nanometer scale organization of metal colloids is important to tailor the properties of nanodevices.[2] Most recent work has focussed on thiolate capped Au[3] and Ag[4] clusters and it was shown that intercluster interaction is possible through the interdigitation of the alkyl chains of adjacent clusters.[5] This interdigitation can lead to superlattice structures.[6] Recently we have shown that Ag nanocrystals form superlattice structures[7] with well defined melting points supporting the conjecture that these superstructures are true molecular materials.[7b]

In an earlier paper[8] we showed that 2-mercaptobenzothiazole (MBT) monolayers on planar gold and silver surfaces have higher thermal stability than the corresponding alkanethiolate monolayers. Interesting observations in this study[8] were the tautomerization of the molecule and differences in the adsorbate orientation on Au and Ag surfaces. MBT adsorbs with its molecular plane perpendicular to the surface on Au, whereas it is parallel on Ag. Surface enhanced Raman spectroscopy (SERS) as well as *ab initio* molecular orbital calculations suggest that MBT adsorbs on Au in the thione form and on Ag in the thiolate form.

This paper describes the synthesis and spectroscopic and calorimetric characterization of MBT capped clusters. These clusters are stable in air for a time scale of several months. This study shows that on different crystallographic planes the orientation of MBT is different. The adsorption is such that close packing of these monolayers is prevented unlike in the case of alkanethiolates. This results in the incorporation of the phase transfer reagent (PTR) on the cluster. Calorimetric observations show irreversible orientational change of the monolayer on these surfaces.

Experimental

MBT capped gold and silver clusters were synthesized using a modified procedure described originally for gold clusters.[3b] Briefly, a 0.0358 M toluene solution of tetra-*n*-octyl ammonium bromide (the PTR) was added to a vigorously stirred 0.0288 M aqueous solution of $HAuCl_4$ ($AgNO_3$ for the silver clusters). After 1 h of stirring, a 0.0139 M toluene solution of MBT was added and the resulting solution was stirred for 10 min. To this an aqueous solution (0.2378 M) of sodium tetrahydroborate was added dropwise over *ca.* 15 min. Reduction and derivatization of the metal is evidenced by the brown color of the toluene phase. The solution was stirred overnight and the organic layer was separated and washed with water to remove unreacted $NaBH_4$. It was allowed to evaporate to 10 ml, and 100 ml of methanol was added in order to precipitate the cluster. The precipitate was allowed to settle and collected by centrifuging. The material was washed several times with methanol to remove unreacted MBT and phase transfer reagent and was air-dried. The products were obtained as black powders which were soluble in non-polar solvents. These clusters are referred to as AuMBT and AgMBT.

Optical absorption spectra were collected in a Varian Cary 5E UV/VIS/NIR spectrophotometer. Solutions were prepared by dissolving the clusters in toluene. Powder X-ray diffractograms were measured with a Shimadzu D1 200 X-ray diffractometer with Co-Kα radiation. The samples were spread on anti-reflection glass slides to give uniform films. The films were wetted with acetone for adhesion and were blown dry before measurement. X-Ray photoelectron spectroscopic measurements were carried out with a VG ESCALAB MkII spectrometer with Mg-Kα radiation. The X-ray flux was kept low (electron power: 70 W) in order to avoid possible beam induced damage. Acquisition took around 15 min for each core level. All regions, C 1s, S 2p, N 1s and Ag 3d (or Au 4f), were measured with 100 eV pass energy. The measurements were carried out under a pressure of 10^{-8} Torr. Thick films of the samples (spread on nickel sample stubs) were used for the measurements. IR spectra were measured with a Bruker IFS 66v FT-IR spectrometer. Samples were prepared in the form of compressed KBr pellets. All spectra were measured with a resolution of 2 cm^{-1} and were averaged over 200 scans. Variable temperature measurements were performed with a home-built heater and a programmable temperature controller. At each temperature the sample was allowed to equilibrate for 10 min before performing the measurements. Electron impact mass spectra were measured with a Finnigan Mat 8230 double sector (*BE* geometry, *B* = magnetic and *E* = electric sectors) mass spectrometer at 70 eV electron impact energy. The

DOI: 10.1039/a909055j

This journal is © The Royal Society of Chemistry 2000

powder samples were introduced through a direct inlet probe and were heated to 623 K at a rate of 100 K min^{-1}. Mass spectra in the range of 50–500 u were measured. At least 100 mass spectra were measured and the scans were averaged for better statistics. Thermogravimetric (TG) data were acquired with a Netzsch STA 409 apparatus. About 10 mg of the sample was used for the measurements conducted in nitrogen atmosphere. Data were measured in the temperature range 298–873 K at a scan speed of 20 K min^{-1}. The samples remaining after mass and TG analysis were metal powders. Differential scanning calorimetry (DSC) data were taken with a Netzsch PHOENIX DSC204 instrument with 10 mg of the sample encapsulated in an aluminium pan. The measurements were conducted in the temperature range 123–473 K at a scan speed of 10 K min^{-1}.

Results and discussion

Fig. 1 shows the absorption spectra of (a) solid MBT, (c) AgMBT and (e) AuMBT in toluene. Spectra in the region 400–800 nm are also shown in an expanded scale. MBT shows an absorption maximum at 328 nm which is blue shifted to 322 nm in AgMBT and to 317 nm in AuMBT. The blue shift of this peak is due to chemisorption at the surface.[9] The band also broadens due to the decrease in the lifetime of the excited state upon adsorption. Adsorption induced changes in the cluster are manifested in the plasmon band, which is red-shifted from 520 to 550 nm for Au and from 430 to 500 nm for Ag. Decreases in intensity as well as the broadness of the bands are attributed to chemisorption.[9] In addition to these two peaks, an additional peak is observed for AgMBT, which we attribute to a charge-transfer transition. It is unlikely that this band is due to the interband transitions in Ag as no similar structure is observed in other Ag clusters.[7] Thus we propose it to be due to charge-transfer excitations. This transition is more prominent in Ag than for Au, and is attributed to the difference in structure of the adsorbate. IR studies show that MBT adsorbs with its molecular plane parallel to the surface on Ag but is almost perpendicular on Au (see below). The geometry of MBT on Ag is due to preferential π bonding.[8] This facilitates charge-transfer from the molecule to the metal, which is almost absent in Au. This also explains the larger blue shift for AuMBT, where the electron donation is only in one direction; from the metal to MBT. In order to ascertain whether the additional transition observed in AgMBT is due to MBT^- species (thiolate) present on the cluster surface, the absorption spectra of MBT in basic solutions were measured. The MBT transition at 328 nm was found to be blue shifted, but no additional transition was observed.

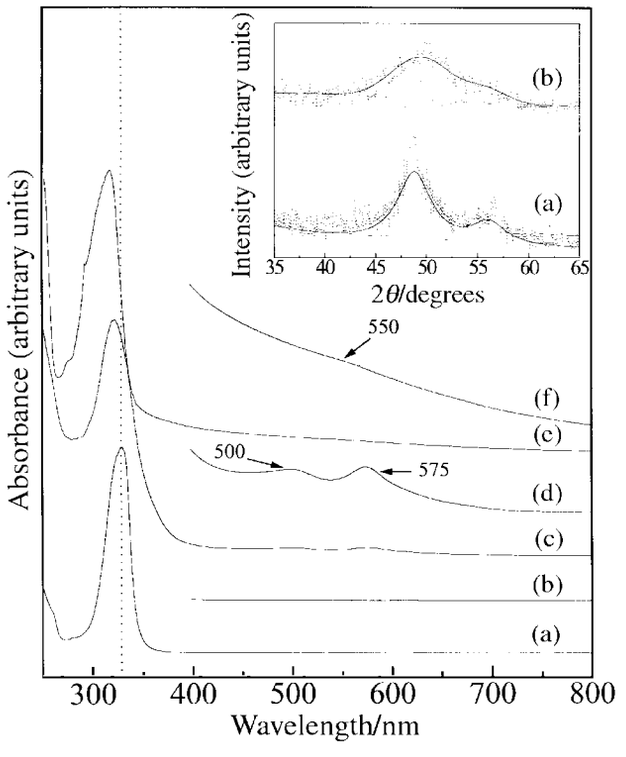

Fig. 1 Optical absorption spectra of solid MBT (a and b), AgMBT (c and d) and AuMBT (e and f) in toluene. In (b), (d) and (f) the absorbance has been multiplied by 50. The peaks of interest are marked. Inset shows the Co-Kα powder diffraction patterns of (a) the Ag and (b) the Au clusters capped with MBT. FWHM of the peaks were calculated from a Gaussian fit of the respective peaks. The components and the fit are also shown. The deviation from the fit for AgMBT is possibly due to a wider distribution of particle sizes.

The inset of Fig. 1 shows the X-ray diffraction patterns of (a) AgMBT and (b) AuMBT. For both, the reflections are broadened compared to bulk Ag or Au reflections indicating the formation of smaller crystallites. In AgMBT, the (111) reflection of Ag is narrower than in Au suggesting a larger particle size. Diameters of the particles were calculated from the XRD line-width using the Scherrer formula[10] which gave 43 ± 5 and 20 ± 5 Å for AgMBT and AuMBT, respectively.

Fig. 2 shows (A) the Ag 3d and (B) the Au 4f regions of the photoelectron spectra of the samples. Au $2f_{7/2}$ and Ag $3d_{5/2}$ signals are observed at 84.0 and 368.2 eV corresponding to Au(0)[3b] and Ag(0)[4a], respectively, as reported previously. The absence of Au(I) and Ag(I) suggests that there is no metal sulfide on the surfaces. An S 2p signal is observed at 164 eV in both the samples (not shown). Two separate features corresponding to two sulfur types are not observed. Both thiol and thione forms of MBT in the solid state would show peaks in the range 163–164 eV and so two distinct features would not be expected at the instrumental resolution (1 eV). We have also observed the S 2p peak at 164 eV for the 2D-SAMs.[8] Likewise, a C 1s peak appeared at 285 eV as in the case of the 2D-SAMs.[8] The N 1s signal appeared at 400 eV (not shown) as reported for adsorbed primary amines.[11]

Mass spectra of AgMBT (A) and AuMBT (B) are shown in Fig. 3. Assignments are listed in Table 1. The peak at *m/z* 254 is due to the presence of the PTR in these clusters. In AgMBT the peak at *m/z* 166 is due to the (MBT−H) ion and the peak at *m/z* 332 is assigned to its dimer. Upon loss of a sulfur atom $(C_{14}N_2S_3)^+$ is formed. An interesting observation in the mass spectrum of AgMBT is that the molecular ion peak is at *m/z* 166, which corresponds to MBT with loss of a proton and

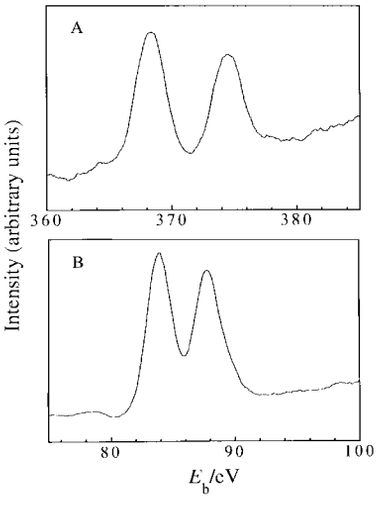

Fig. 2 (A) Ag 3d and (B) Au 4f X-ray photoelectron spectra of AgMBT and AuMBT, respectively.

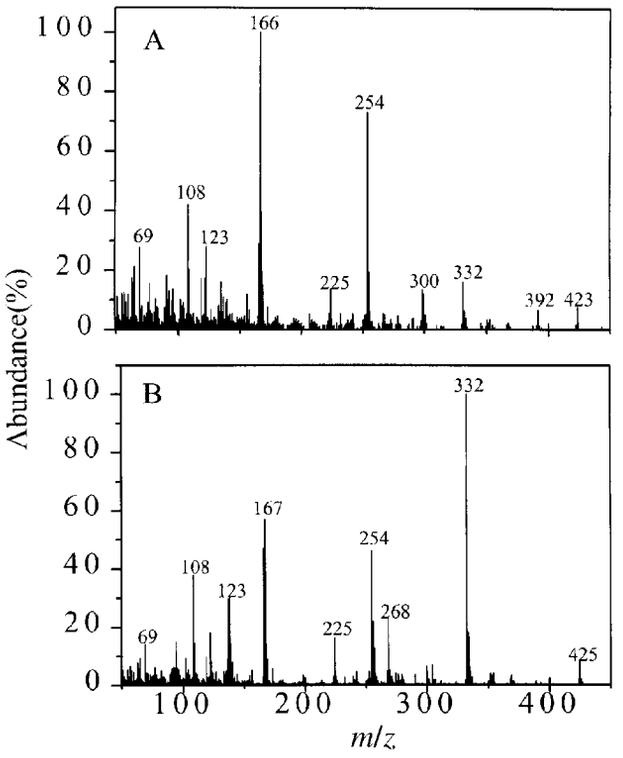

Fig. 3 Mass spectra of (A) AgMBT and (B) AuMBT. Peaks of interest are marked. Assignments of the peaks with possible structures are given in Table 1.

suggests that MBT is in the thiolate form on the Ag surface. For Au a peak at *m/z* 167 is present along with a peak at *m/z* 166, which is consistent with adsorption in the thione form (see below). Whereas the MBT ion is the 100% (base) peak in AgMBT, the corresponding base peak for AuMBT is the dimer. This is attributed to the difference in the adsorption geometry, which makes dimer formation facile for AuMBT. The presence of the molecular ion of MBT (*m/z* 167) along with the peak at *m/z* 332 on the Au surface suggests that the dimer is not desorbed directly from the surface but is formed as a result of association reactions in the gas phase.

Fig. 4 shows the IR spectra of (a) solid MBT, (b) AgMBT and (c) AuMBT. Peak positions and assignments are given in Table 2. All the peaks are downshifted on the clusters suggesting that only adsorbed MBT is present. The 3077 cm^{-1} band in solid MBT is attributed to the aromatic CH stretching. This band is red shifted to 3061 cm^{-1} in Au and is almost absent in Ag. This behavior is understood in terms of the IR selection rule, which states that only those vibrations whose dipole moments are perpendicular to the surface are excited. The aromatic C–H stretching is parallel to the Ag surface and hence it is not excited. For Au, however, the aromatic C–H may be perpendicular to the surface. From this it is concluded that a major fraction of MBT adsorbs on Ag with an almost parallel geometry and on Au with a near perpendicular geometry. These geometries are the same as found for the corresponding 2D-SAMS.[8] Use of the surface IR selection rule should, however, be made with caution for these samples because of random orientation of the clusters and the non-polarized nature of the IR radiation. A closer examination of all the peaks suggests that the surface selection rule can be applied to monolayers on clusters as orientational differences are also seen in the low wavenumber in-plane modes. The broadness of the bands suggests chemisorption of the molecule on the surface. The presence of symmetric and antisymmetric CH_2 and CH_3 vibrations indicate the incorporation of the phase transfer reagent on the cluster. Each phase transfer

Table 1 Mass spectral features and assignments

m/z	Formula	Structure
332	$(C_{14}S_4N_2H_8)^+$	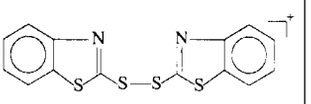
300	$(C_{14}S_3N_2H_8)^+$	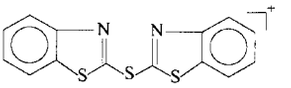
225	$(C_8S_3N_2H_5)^+$	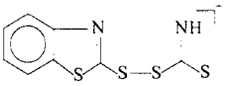
167	$(C_7S_2NH_5)^+$	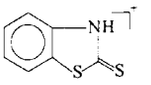
166	$(C_7S_2NH_4)^+$	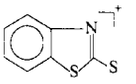
123	$(C_6SNH_5)^+$	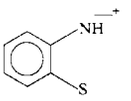
108	$(C_6SH_5)^+$	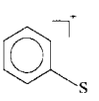

reagent molecule has 28 CH_2 groups and 4 CH_3 groups while for each MBT, there are only four aromatic C–H bonds contributing to the intensity. Furthermore, aromatic C–H stretching modes are an order of magnitude weaker than the aliphatic modes.

In the low wavenumber region, the in-plane C–C stretching at 1595 cm^{-1} in solid MBT is red shifted to 1582 cm^{-1} in Au and is almost absent in Ag. Again this is attributed to the parallel orientation on Ag and perpendicular orientation on Au. We observed a substantial difference in the 1426 cm^{-1} band of MBT upon adsorption. Whereas this band is very strong in Ag and undergoes splitting, it is only of medium intensity on Au. The ν(C–S) mode of MBT is present at 603 cm^{-1} while on Ag this appears as a doublet. The 689 cm^{-1} band on Ag and 698 cm^{-1} band on Au are due to C–S stretching of the heterocyclic ring system,[8] which is not distinctly clear in solid MBT. This mode is also present in the SER spectrum of the 2D-SAM.[8] These peaks are not due to the PTR, as ascertained independently.

From the IR studies we deduce that there is an orientational difference for MBT monolayers on Au and Ag cluster surfaces and this difference is similar to that in 2D-SAMs. These monolayers show high thermal stability on 2D surfaces of Au and Ag. Annealing of the metal islands results in close packing of the monolayers in defined areas. Even though the molecule has different adsorption sites (two sulfurs and one nitrogen), the temperature dependent dynamics on the 2D surfaces were minimal. This is attributed to strong surface binding or dense self-assembly.[8] Since such a dense assembly is absent for the cluster surfaces here as evidenced by the incorporation of PTR,

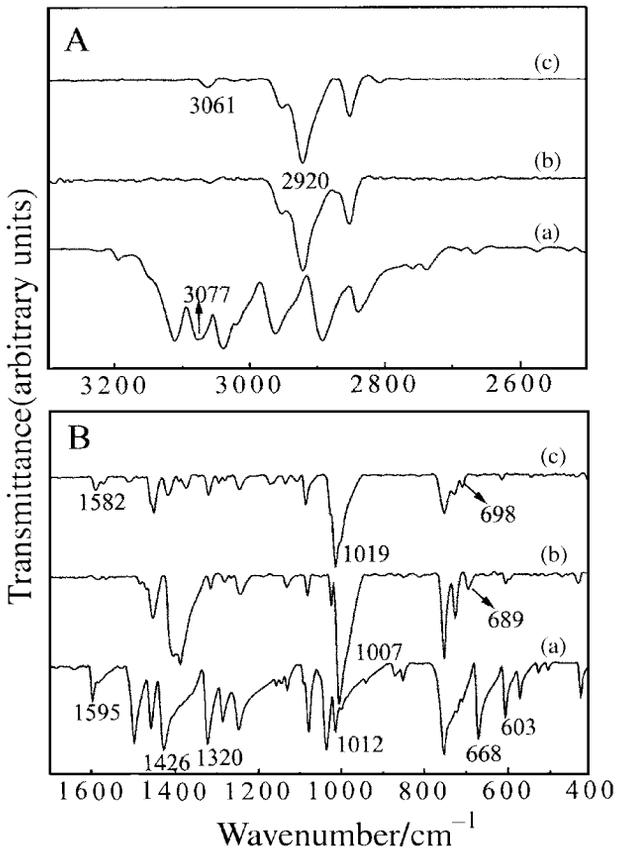

Fig. 4 (A) High and (B) low wavenumber FTIR spectra of (a) solid MBT (b) AgMBT and (c) AuMBT. Peak positions and assignments are given in Table 2.

Table 2 IR wavenumbers (in cm^{-1}) and assignments of MBT as a solid and MBT capped. Au and Ag clusters

Assignment[a,b]	MBT solid	MBT on Au	MBT on Ag
	3111		
νCH	3077	3061	
νCH	3038		
νCH	2961		
	2891		
	2839		
νCC	1640		
νCC_{ip}	1595	1582	
νCN		1541	
νCC	1496	1503	
νCC_{ip}	1456	1453, 1445	1449
νCC	1426	1411	1403, 1385
		1366	
νCN	1320	1312	1310
νCC	1283	1287	1276
νCC	1245		
δCH		1237	1238
δCH_{ip}	1148	1161	
δCH	1125	1127	1126
δCH_{ip}	1076	1099	1076
δCH_{ip}		1078	
νCN	1034		
δCCC	1012		1019
δCH		1007	
δCH			1002
δCH	949		
δCH_{op}	867		868
δCH_{op}	751	745	748
δCH			721
νCS		698	689
νCS	668		
νCS	603	605	603

[a] $_{ip}$ Refers to the in-plane and $_{op}$ refers to the out of plane vibrations respectively, δ-bending, and ν-stretching vibrations. [b]Ref. 12.

hence variable-temperature IR spectra should show significant changes.

Fig. 5 shows variable-temperature IR spectra of AgMBT in (A) the high and (B) low wavenumber regions. The prominent peaks in the high wavenumber region show a gradual blue shift with increasing temperature. In the room temperature spectrum, the methylene symmetric mode (d^+) is present at 2920 cm^{-1}, which is shifted to 2925 cm^{-1} at higher temperature. This arises from the PTR molecule, which is in a state of low rotational freedom at room temperature, but gains internal energy at increased temperature and the population of the rotating phase increases. Along with this shift, the peak intensity reduces gradually. Since MBT is flat on the surface, the aromatic C–H stretches are not observed.

The bands at 1403 and 1385 cm^{-1} undergo an intensity reversal at high temperatures which appears to be gradual and no shift in positions is observed. An interesting observation is that the spectrum remains essentially unchanged up to 453 K, except for the intensity reversal above. However, at 473 K dramatic changes occur with the C–S stretching at 690 cm^{-1} disappearing and new peaks emerging at 1425 and 1491 cm^{-1}. Other differences observed are in the peak at 1002 cm^{-1}, which is reduced in intensity along with the emergence of a peak at 1030 cm^{-1}, which is attributed to C–N stretching. All these together can be attributed to the coexistence of other possible adsorbate geometries. Similar changes have also been observed in the Ag 2D-SAMs.[8] Trace (i) in Fig. 5 shows the spectrum after cooling back from 473 K. Since there are differences between the spectra of the as prepared sample and after cooling back from 473 K the adsorbate geometry appears to undergo an irreversible change upon heating.

In contrast with the AgMBT cluster and 2D-SAMs, the temperature dependent dynamics of the AuMBT cluster is more dramatic. Fig. 6A shows the C–H stretching region of the AuMBT cluster spectra where the peak at 3061 cm^{-1} due to aromatic C–H stretching disappears at 398 K due to the change in adsorbate geometry as the temperature increases. The MBT molecule, which was perpendicular to the surface at room temperature, appears to fall onto the surface at higher temperatures. As a result of this, the C–H stretching mode becomes parallel to the surface and is not excited. The methylene stretching modes show a gradual blue shift with temperature as found for the Ag cluster. Fig. 6B shows the low wavenumber region of AuMBT spectra at various temperatures. A sudden transition is observed at 373 K. Changes at this temperature include the decreased intensity of the 1582 cm^{-1} band attributed to in-plane C–C stretching and the intensity reversal of 1453 and 1445 cm^{-1} bands which ultimately merge and blue shift. At 373 K, the 1366 cm^{-1} band broadens and merges into the 1411 cm^{-1} band and at 398 K this band disappears along with the 1582 cm^{-1} band. In addition, a new peak emerges at 1032 cm^{-1} attributed to the C–N stretching of MBT.[8] At 373 K a new peak emerges at 665 cm^{-1} which undergoes a red shift to 653 cm^{-1} at higher temperatures. The 605 cm^{-1} band is red shifted and broadened at 373 K but returns to its original position at 398 K. These peaks are attributed to C–S stretching.

We explain these changes in the following manner: along with MBT, PTR also is present on the cluster surface, as the temperature is increased to 373 K, the alkyl chain of the PTR becomes more disordered and as a result, MBT molecules fall onto the cluster surface with their molecular planes parallel to it. This is evidenced by the disappearance of the 1582 cm^{-1} $\nu(C–C)_{ip}$ and aromatic C–H stretching modes. Along with this change in adsorbate geometry, the MBT molecule undergoes a structural transition which appears to be driven by tautomerization and explains the emergence of new peaks.

The spectrum after cooling is shown in trace (i), which differs

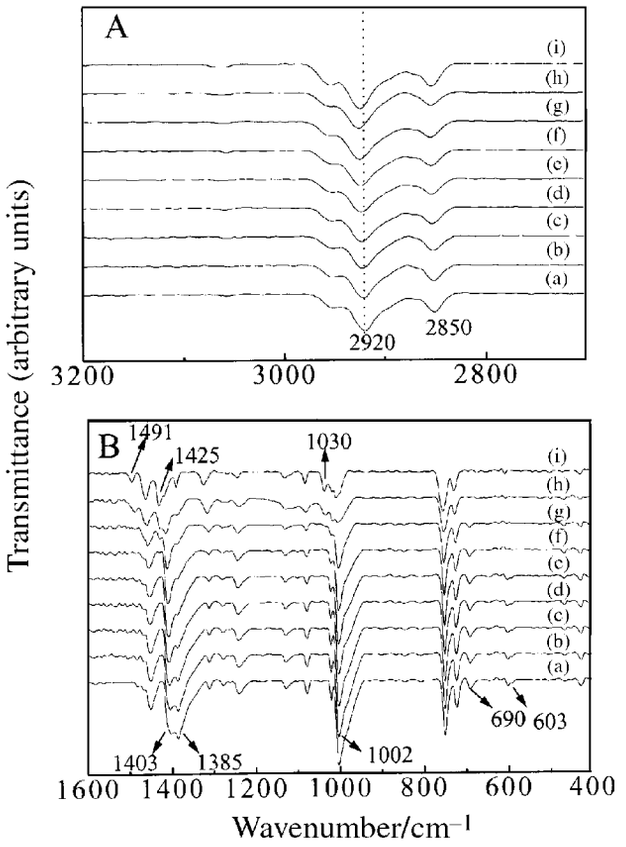

Fig. 5 Variable temperature FTIR spectra for AgMBT in (A) the high wavenumber and (B) the low wavenumber region. The temperatures are: (a) 298, (b) 323, (c) 348, (d) 373, (e) 398, (f) 423, (g) 448, (h) 473 K and (i) cooling back to 298 K, respectively.

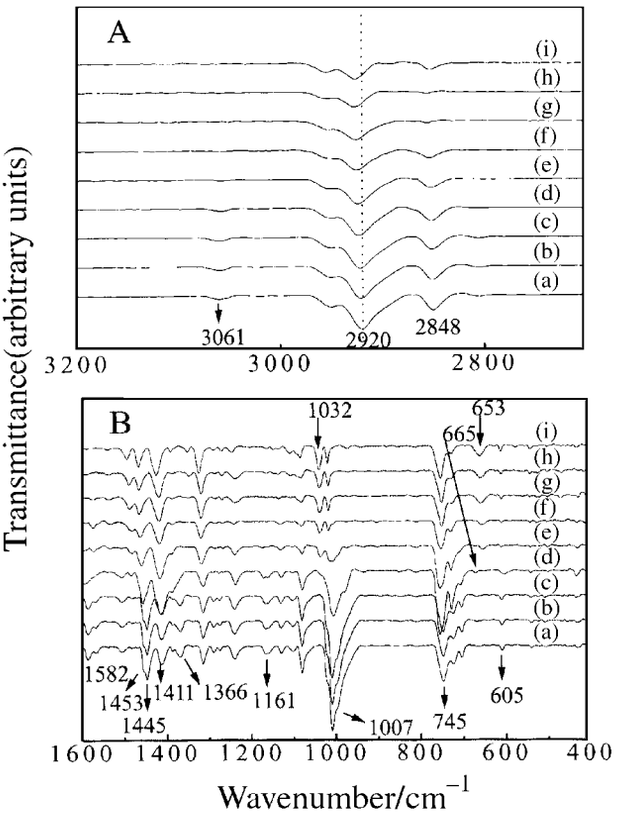

Fig. 6 Variable temperature FTIR spectra for AuMBT in (A) the high wavenumber and (B) the low wavenumber region. The temperatures are: (a) 298, (b) 323, (c) 348, (d) 373, (e) 398, (f) 423, (g) 448, (h) 473 K and (i) cooling back to 298 K, respectively.

from trace (a). There are a number of additional bands, rationalized by different adsorption geometries present on the surface. Again the absence of aromatic CH stretching and the low intensity of in-plane bands suggests that after cooling, MBT molecules do not return to their original perpendicular orientation.

Fig. 7 shows the DSC trace of AuMBT, which shows an exotherm at 415 K attributed to the change in orientation and to tautomerization. The transition temperature and enthalpy of AuMBT in the heating cycle are 415 K and 49.8 J g^{-1}, respectively. In the cooling cycle, no transition is observed. This indicates that the structural change is not reversible as also evidenced from the variable temperature IR data. Even though the phase transfer reagent is present on the surface of the cluster, no endotherm peak corresponding to its melting was observed in the temperature range investigated. It has been reported that the melting of octanethiol occurs at low temperatures in octanethiol capped Au clusters.[5] From the IR data we note that the alkyl chains of PTR acquire rotational freedom gradually and that no sudden transition is observed. Thus DSC gives corroborative evidence for the orientational change of MBT at higher temperature. AgMBT also shows a broad exotherm (not shown) at the same temperature, but the enthalpy is low (16.5 J g^{-1}) compared to the Au cluster. This lower value suggests that the structural transition is not as significant as in AuMBT.

The inset of Fig. 7 shows thermogravimetric data for (a) AuMBT and (b) AgMBT, which show a two step decomposition. This is attributed to the presence of different orientations of the molecule on the surface. On both Au and Ag, different orientations are present, although the perpendicular structure is dominant on Au and the parallel one on Ag. In the flat geometry, there is preferential π bonding between the surface and the adsorbate. As a result of this, it is likely that the perpendicular structure desorbs from the surface first followed by the flat structure. Thus for AuMBT one should observe a large mass loss for the first step, and a small loss for the second step (Δm_1 and Δm_2, respectively) whereas the reverse behavior should be observed for Ag. This is observed (Fig. 7); on AgMBT the mass loss at low temperature (524 K) is lower, which is due to desorption of perpendicular geometry molecules and at 588 K it is higher which is due to desorption of the parallel geometry molecules (Δm_1 and Δm_2, respectively). By contrast, for AuMBT, the mass loss at 526 K is higher (perpendicular geometry) and that at 603 K is lower (parallel geometry). In both cases the mass losses are low, compared to

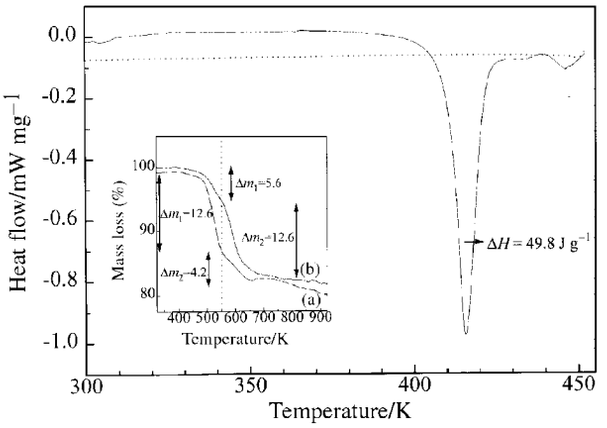

Fig. 7 Differential scanning calorimetric traces of AuMBT. The full line (—) represents heating cycle and the dashed line shows the cooling cycle (- - -). The enthalpy of transition is indicated. The inset shows TGA curves of (a) AuMBT and (b) AgMBT. Mass losses are indicated.

alkanethiolate capped clusters. The mass loss shows some contribution from the phase transfer reagent; however, this appears to be small. The differences in adsorption geometry are manifested in the TG traces since the heating rate is faster than the orientational changes, which occur below 400 K as revealed by IR.

Summary and conclusions

This study has shown that MBT adsorbs with its molecular plane flat on Ag and perpendicular on Au. Surface enhanced Raman spectroscopic investigations of the MBT monolayers on planar gold and silver surfaces also led to the same conclusions. On the cluster surface the monolayer structure is an admixture of both the orientations but the predominant structure is that found on the 2D-SAMS. The monolayer is less organized than on 2D-SAMS and the phase transfer reagent is incorporated at defect sites. Whereas the temperature dependent dynamics is minimal on 2D-SAMs, it is significant on the cluster surfaces, especially on the Au cluster. Variable temperature IR studies show that above 373 K, the MBT monolayer on the Au surface undergoes a structural transition, which is driven by tautomerization. This is evidenced by the emergence of new bands in the spectra. Moreover, the adsorbate geometry also changes from a predominantly perpendicular to parallel orientation on Au cluster surfaces at higher temperatures. This is manifested by the disappearance of the aromatic C–H stretching and in-plane modes. Correspondingly DSC shows an exotherm around this temperature.

Mass spectral data shows that MBT adsorbs on Ag in the thiolate form, *i.e.*, with loss of a proton, whereas on Au, it is present as the thione. This together with the perpendicular geometry favors dimer formation with loss of a hydrogen molecule upon desorption. It is interesting that the MBT monolayer shows a charge-transfer band in the optical absorption spectrum, not observed with other capping molecules. This band is readily observed only on the Ag surface probably because of the parallel geometry on the surface, which favors electron donation from the monolayer to the metal.

Acknowledgements

T. P. thanks the Department of Science and Technology, Government of India, for funding his research programme on SAMs. N. S. thanks the Council of Scientific and Industrial Research, New Delhi for the award of a research fellowship.

References

1 G. Schon and U. Simon, *Colloid Polym. Sci.*, 1995, **273**, 101; G. Schon and U. Simon, *Colloid Polym. Sci.*, 1995, **273**, 202.

2 R. P. Andres, T. Bein, M. Dorogi, S. Feng, J. I. Henderson, C. P. Kubiak, W. Mahoney, R. G. Osifchin and R. Reifenberger, *Science*, 1996, **272**, 1323; A. N. Shipway, M. Lahav, R. Blonder and I. Willner, *Chem. Mater.*, 1999, **11**, 13.

3 (*a*) M. J. Hostetler and R. W. Murray, *Curr. Opin. Colloid Interface Sci.*, 1997, **2**, 42; (*b*) M. Brust, M. Walker, D. Bethell, D. J. Schiffrin and R. Whyman, *J. Chem. Soc., Chem. Commun.*, 1994, 801; (*c*) M. J. Hostetler, J. E. Wingate, C.-J. Zhong, J. E. Harris, R. W. Vachet, M. R. Clark, J. D. Londono, S. J. Green, J. J. Stokes, G. D. Wignall, G. L. Glish, M. D. Porter, N. D. Evans and R. W. Murray, *Langmuir*, 1998, **14**, 17; (*d*) R. H. Terril, T. A. Postlethwaite, C.-H. Chen. C.-D. Poon, A. Terzis, A. Chen, J. E. Hutchison, M. R. Clark, G. Wignall, J. D. Londono, R. Superfine, M. Falvo, C. S. Johnson, E. T. Samulski Jr. and R. W. Murray, *J. Am. Chem. Soc.*, 1995, **117**, 12537; (*e*) M. Brust, J. Fink, D. Bethell, D. J. Schiffrin and C. Kiely, *J. Chem. Soc., Chem. Commun.*, 1995, 1655; (*f*) D. V. Leff, P. C. Ohara, J. R. Heath and W. M. Gelbart, *J. Phys. Chem.*, 1995, **99**, 7036; (*g*) D. V. Leff, L. Brandt and J. R. Heath, *Langmuir*, 1996, **12**, 4723; (*h*) M. J. Hostetler, J. J. Stokes and R. W. Murray, *Langmuir*, 1996, **12**, 3604; (*i*) S. R. Johnson, S. D. Evans, S. W. Mahon and A. Ulman, *Langmuir*, 1997, **13**, 51; (*j*) M. M. Alvarez, J. T. Khoury, T. G. Schaaff, M. N. Shafigullin, I. Vezmar and R. L. Whetten, *J. Phys. Chem. B*, 1997, **101**, 3706.

4 (*a*) S. Y. Kang and K. Kim, *Langmuir*, 1998, **14**, 226; (*b*) S. A. Harfenist, Z. L. Wang, M. M. Alvarez, I. Vezmar and R. L. Whetten, *J. Phys. Chem.*, 1996, **100**, 13904.

5 A. Badia, S. Singh, L. Demers, L. Cuccia, G. R. Brown and R. B. Lennox, *Chem. Eur. J.*, 1996, **2**, 359.

6 C. P. Collier, T. Vossmeyer and J. R. Heath, *Annu. Rev. Phys. Chem.*, 1998, **49**, 371; J. R. Heath, C. M. Knobler and D. V. Leff, *J. Phys. Chem. B*, 1997, **101**, 189; S. A. Harfenist, Z. L. Wang, M. M. Alvarez, I. Vezmar and R. L. Whetten, *J. Phys. Chem.*, 1996, **100**, 13904; Z. L. Wang, *Adv. Mater.*, 1998, **10**, 13; X. M. Lin, C. M. Sorensen and K. J. Klabunde, *Chem. Mater.*, 1999, **11**, 198.

7 (*a*) N. Sandhyarani, M. R. Resmi, R. Unnikrishnan, Shuguang Ma, K. Vidyasagar, M. P. Antony, G. Panneer Selvam, V. Visalakshi, N. Chandrakumar, K. Pandian, Y. T. Tao and T. Pradeep, *Chem. Mater.*, 2000, **12**, 104; (*b*) N. Sandhyarani, M. P. Antony, G. Panneer Selvam and T. Pradeep, *Langmuir*, submitted; (*c*) N. Sandhyarani, T. Pradeep, J. Chakrabarti, M. Yousuf and H. K. Sahu, *Phys. Rev. B*, 2000, in press.

8 N. Sandhyarani, G. Skanth, S. Berchmans, V. Yegnaraman and T. Pradeep, *J. Colloid Interface Sci.*, 1999, **209**, 154.

9 A. Henglein, *J. Phys. Chem.*, 1993, **97**, 5457.

10 A. R. West, *Solid State Chemistry and its Applications*, John Wiley and Sons, New York, 1987.

11 D. Briggs and M. D. Seah, *Practical Surface Analysis by Auger and X-ray Photoelectron Spectroscopy*, John Wiley and Sons, Chichester, 1984.

12 A Raman study of mercaptobenzimadazole has been carried out: S. Mohan, N. Sundaraganesan and J. Mink, *Spectrochim. Acta, Part A*, 1991, **47**, 1111.

Paper a909055j